Investigating the Effects of Operating Parameters on Hydroxy Gas Production through Solar-Powered Alkaline Water Electrolysis: a COMSOL Simulation and Experimental Approach

Liaquat Ali Khan[a] | Muhammad Bilal Arshad[b,*] | Ali Raza[b]

[a] Marine Engineering Department Military Technological College, Muscat
[b] Department of Mechanical Engineering, National University of Technology Islamabad, Pakistan

* Corresponding author, Email: bilalarshad6920@gmail.com

Abstract

Depletion of conventional fossil fuels poses a significant concern, especially in transportation, where demand exceeds the production rate, hence, risk of fuel crisis. Fossil fuel combustion also heavily pollutes the environment, impacting global quality of life. Therefore, renewable and clean energy alternatives are urgently needed for sustainability. Hydrogen energy, particularly when sourced from renewable power like solar or wind, presents a promising solution. This study explores a unique approach to hydrogen production through a solar-powered alkaline electrolyzer, using both simulation and experimental testing to optimize its efficiency. The study uses COMSOL Multiphysics to simulate various operating conditions, which were then validated experimentally. Key operating parameters such as electrode spacing, electrolyte concentration, and temperature were systematically adjusted to identify conditions that maximize gas output. An innovative control system monitored and regulated the gas pressure, automatically shutting off the electrolyzer at 1.8 bars to ensure safety and efficiency. Findings highlight how close electrode spacing, higher electrolyte concentration, and elevated temperatures significantly boost hydrogen production.

1 Introduction

The growing need of fossil fuels and their possible scarcity in future make finding renewable energy resources crucial. With the increase in global warming and other environmental concerns, developing and managing sources like wind and solar power is essential. [1] If using fossil fuels is continued at the current rate, it is estimated they will run out by 2060. New reserves may be discovered, delaying this timeline, or rate of increase in fuel usage further in future might result in early depletion causing serious industrial and transportation problem due to fuel scarcity. But to keep global warming to a relatively safe level of $2\,°\mathrm{C}$ by 2050, it is need of time to find alternative and clean energy sources [2].

Hydrogen is an excellent energy storage medium due to its high gravimetric energy density of about $140\,\mathrm{MJ/kg}$, it is more than double that of typical solid fuels, which have around $50\,\mathrm{MJ/kg}$. When hydrogen burns, it produces water, making it an environmentally friendly energy source. Hydrogen energy is considered synonymous with sustainable energy as it can replace fossil fuels and hydrocarbons. However, hydrogen systems are truly clean and sustainable, only when the hydrogen is being produced using renewable energy sources. [3]

Besides the attractive properties of hydrogen as a fuel it has several problems associated with its production, storage and transportation. Currently, about 70 million tons of hydrogen has been produced globally each year, with the majority coming from fossil sources. Specifically, 76% is derived from natural gas through steam methane reforming, and 22% comes from coal via gasification. Only about 2% is produced using water electrolysis [4].
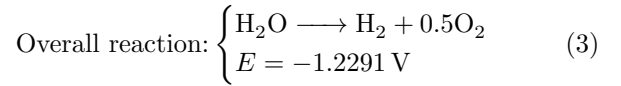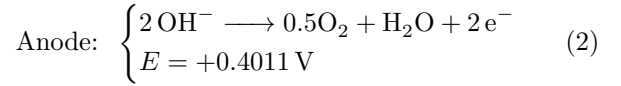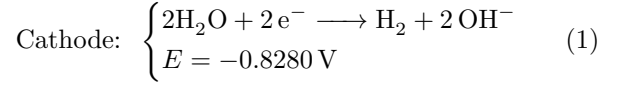
Due to the very low density of hydrogen gas, it is very difficult to store it without leaking. Storing the gas is only possible under two conditions:

- Storing it at very high pressures in specially manufactured vessels.
- Storing it in liquid phase at cryogenic conditions at temperature below $-260\,°\mathrm{C}$.

Both methods are not cost effective, that's why there is a need of a process which overcome these limitations in a cost-effective manner. In alkaline electrolysis, the electrodes are submerged in a 20-40 wt. % potassium hydroxide solution and separated by a diaphragm or membrane to keep the evolved product gases isolated.

Equations (1) to (3) present the half-cell and overall reactions along with their electrode potentials against a standard hydrogen electrode at 298.15 K and pH

13.996 [5].

$$\text{Cathode:} \begin{cases} 2\mathrm{H_2O} + 2\,\mathrm{e}^- \longrightarrow \mathrm{H_2} + 2\,\mathrm{OH}^- \\ E = -0.8280\,\mathrm{V} \end{cases} \quad (1)$$

$$\text{Anode:} \begin{cases} 2\,\mathrm{OH}^- \longrightarrow 0.5\mathrm{O_2} + \mathrm{H_2O} + 2\,\mathrm{e}^- \\ E = +0.4011\,\mathrm{V} \end{cases} \quad (2)$$

$$\text{Overall reaction:} \begin{cases} \mathrm{H_2O} \longrightarrow \mathrm{H_2} + 0.5\mathrm{O_2} \\ E = -1.2291\,\mathrm{V} \end{cases} \quad (3)$$

Due to the difference in consumption and production of water in the half cells, an electrolyte concentration gradient is formed. To compensate for this difference in electrolyte concentration, the anodic and cathodic electrolyte cycles are continuously mixed. However, this cycling strategy restricts the typical operation range to 10-40% of the nominal load, [6, 7], as oxygen purity is significantly reduced by hydrogen contamination below this limit. This contamination arises from diffusion through the separator and the mixing of the gas-saturated electrolyte solution, which allows the dissolved species to reach the opposite gas separator. Consequently, industrial electrolyzer's are shutdown when a foreign gas content of 2% vol. is detected in the exhaust [8] which corresponds to about 50% of the explosion limit of $\mathrm{H_2/O_2}$ mixtures [9]. This issue is particularly important when the electrolyzer is coupled with a renewable energy source and operated in the low current density range [10].

Kothari, Buddhi, and Sawhney (2008) [11] present a comprehensive analysis of various hydrogen production methods, emphasizing both environmental and economic factors. Hydrogen technology is gaining prominence as a viable solution to mitigate climate change and address fossil fuel depletion. This review compares conventional and alternative energy sources for hydrogen production, including natural gas, coal, nuclear, biomass, solar, and wind, by examining 14 different production methods in terms of their technical and economic aspects.

Chi and Yu (2018) [3] review the role of hydrogen as an energy storage medium, emphasizing its growing relevance due to the surplus power generated from renewable sources like wind and solar energy. The review compares various water electrolysis technologies, including alkaline water electrolysis, proton exchange membrane (PEM) water electrolysis, solid oxide water electrolysis, and alkaline anion exchange membrane (AAEM) water electrolysis Martín et al. (2019) [12] discuss the growing emphasis on reducing greenhouse gas emissions without compromising modern lifestyles, highlighting the role of renewable energy sources and hydrogen-based storage and transportation systems. The paper reviews existing hydrogen production tech-

niques with a particular emphasis on electrolysis, a mature and well-established method. Electrolysis, especially alkaline water electrolysis, is presented as a viable approach due to its potential for integration with renewable energy sources. The authors explore various proposals that serve as preliminary steps towards a hydrogen economy, demonstrating the feasibility and benefits of transitioning to green hydrogen production.

Ishaq and Dincer (2021) examine three renewable energy-based configurations for hydrogen production, focusing on solar photovoltaic (PV), geothermal power, and biomass gasification. The study includes a novel biomass gasification setup utilizing multistage water gas shift reactors. Each hydrogen production method is analyzed using different simulation tools: EES software for solar PV and geothermal systems, and Aspen Plus for biomass gasification [13]. Boretti (2020) reviews recent advancements in the power density and efficiency of hydrogen (H_2) internal combustion engines (ICEs), focusing on dual-fuel and H_2-only systems. The paper highlights the potential of dual-fuel direct injection (DI) diesel-H_2 compression ignition (CI) engines and H_2-only positive ignition (PI) engines, including DI and jet ignition (JI) technologies. These systems are projected to achieve peak efficiencies around 50%, with peak power efficiencies exceeding 46% and driving cycle average efficiencies above 35%, especially when integrated into hybrid powertrains [14].

Zareei et al. (2014) find that adding up to 15% hydrogen to CNG increases burn speed and peak heat release, with optimal ignition timing adjusted to maximize peak pressure. This blend also raises maximum in-cylinder temperatures to around 150 K at 8° crank angle [15].

The literature lacks controlled and dynamic model estimations of alkaline electrolyzers operated with renewable energy sources. Therefore, this study investigates a solar-powered controlled electrolyzer under various operating conditions, validating the simulation results through experimental data. Additionally, a control system is designed and evaluated to provide a uniform on-demand hydrogen and oxygen blend supply to the engine, with the effects of this blending examined experimentally.

2 Methodology

A thorough review of existing research on using renewable energy to produce hydrogen through electrolysis was conducted to build on existing knowledge and identify areas for improvement. Following this, an electrolyzer model has been designed and simulated in COMSOL®software. After this, an experimental setup was designed to enhance the performance of the elec-

trolysis cell. A 200-watt solar power system was utilized to operate the electrolyzer. Key parameters, such as the concentration of potassium hydroxide (KOH) in solution, temperature, number of plates, and distance between plates, were varied to achieve optimal gas production within a specific timeframe. The study also focused on the simulation and experimental analysis of an alkaline electrolyzer powered by solar energy to produce hydrogen and oxygen gases. Detailed mathematical modeling was essential for calculating design parameters and optimizing the electrolysis process. The water electrolysis reaction, energy requirements, and voltage decomposition were analyzed, accounting for various losses. Faraday's law was used to determine gas production rates, with mole flow rates converted to volume flow rates using the ideal gas equation.

In the experimental setup, different concentrations of KOH and elevated temperatures were tested to assess their impact on gas output. Different materials were tested to evaluate their effectiveness in withstanding the corrosive environment. A control system was designed to monitor the pressure within the gas container. When the pressure reached 2 bars, a blow valve will be open, cutting off the connection to the electrolyzer. Additionally, the power generated by the solar panel was stored in a 12-volt, 20 Ah battery to ensure a continuous power supply. Simple and cost-effective designs were prioritized, and various materials were tested to select the most suitable ones for optimal performance.

3 Mathematical Modeling

A careful approach was taken to calculate the design parameters and create a mathematical model for controlled water electrolysis using solar energy. In this section specific design parameters chosen for the machine mechanisms and the reasons for each choice are explained in detail. This helps to ensure a clear understanding of the design decisions. Additionally, necessary calculations were done to find these design parameters and determine the power requirements for this study. These calculations are important to make sure the mechanism works well and meets the energy requirement of the solar hydrogen electrolysis system.

3.1 Modeling of electrolyzer

Water electrolysis is a process of using electricity to split water into hydrogen and oxygen gas. The complete reaction is:

$$2H_2O(\text{liq}) + \text{electrical energy} \longrightarrow 2\,H_2(g) + O_2(g) \tag{4}$$
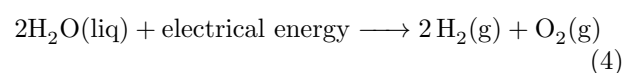
At the cathode, where electrons enter the water, hydrogen ions (H^+) are reduced to hydrogen gas (H_2). The reaction at the cathode is:

$$4\,H^+(aq) + 4\,e^- \longrightarrow H_2(g) \tag{5}$$
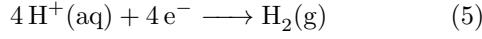
At the anode, where electrons leave the water, water molecules (H_2O) are oxidized to oxygen gas (O_2) and hydrogen ions (H^+). The reaction at the anode is:

$$2\,OH^- \longrightarrow H_2O + \frac{1}{2}\,O_2(g) \tag{6}$$
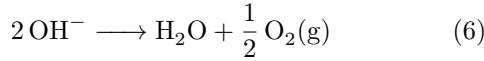
Required energy is given by Gibbs-Helmholtz equation:

$$\Delta G_R = \Delta H_R - T\,\Delta S_R \tag{7}$$

Water splitting is a thermodynamically which is a non-favorable reaction

$$\Delta H_R = [\Delta H_R(\text{Products}) - \Delta H_R(\text{Reactants})]\,, \tag{8}$$
$$\Delta H_R = [285\,\text{kJ/mol} - (0+0)]\,,$$
$$\Delta H_R = 285.83\,\text{kJ/mol}\,, \tag{9}$$
$$W = P\,\Delta V\,, \tag{10}$$
$$W = (101.3 \times 10^3\,\text{Pa}) \times (1.5\,\text{mol})$$
$$\times \left(22.4 10^{-3}\,\frac{\text{m}^3}{\text{mol}}\right) \times \left(\frac{298.15\,\text{K}}{273.15\,\text{K}}\right) = 3.23\,\text{kJ}\,, \tag{11}$$
$$\Delta H_R = \Delta U + p\,\Delta V\,, \tag{12}$$
$$\Delta H_R = 282.1\,\text{kJ} + 3.72\,\text{kJ} = 285.83\,\text{kJ/mol}\,. \tag{13}$$

$T\Delta S_R$ can be found from environment because ΔS is always greater than zero. Hence,

$$\Delta G_R = \Delta H_R - T\,\Delta S_R\,, \tag{14}$$
$$\Delta G_R = (285.83\text{–}48.7)\,\text{kJ/mol} = 237.13\,\text{kJ/mol}\,. \tag{15}$$

At standard temperature and pressure, $T = 298.15\,\text{K}$ and $P = 1.013\,\text{atm}$. For water electrolysis reaction, $\Delta G_R = 237.13\,\text{kJ/mol}$. Voltage required for decomposition is given by:

$$\Delta G_R = -z\,F\,U\,, \tag{16}$$
$$U = \frac{\Delta G_R}{Fz}\,, \tag{17}$$
$$U = \frac{-273.13\,\text{kJ/mol}}{2 \times 96485\,\text{A}\cdot\text{sec/mol}} = -1.23\,\text{volts}\,. \tag{18}$$

This decomposition voltage depends on aggregate state of reactant and temperature. In order to incorporate the effect of losses during the electrolysis process different types of losses are added. Frictional losses which occur due to the surface resistance and the drop of voltage due to electrical resistance and over potential.

$$V_{\text{cell}} = V_{\text{rev}} + V_{\text{act,cathode}} + V_{\text{act,anode}} \tag{19}$$

The more the current the more the losses [16]. Now to get the amount of gas produced Faradays law of electrolysis is used [17]:

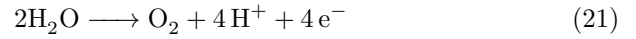$$n = \text{Molar flow rate of hydrogen} = \frac{It}{zF}\,, \tag{20}$$

where

n : Amount (mol) I : Current (A) t : Time (s)

z : No of electrons

F : Faraday Constant (96485 C/mol)

Oxidation reaction occures at Anode:

$$2H_2O \longrightarrow O_2 + 4\,H^+ + 4\,e^- \tag{21}$$
$$n(O_2) = \frac{0.1\,\text{A} \times 60\,\text{sec}}{4 \times 96485\,\text{C/mol}} = 1.55 \times 10^{-5}\,\text{mol}\,. \tag{22}$$

Reduction reaction will takes place at cathode

$$2H^+ + 2e^- \longrightarrow H_2 \tag{23}$$
$$n(H_2) = \frac{0.1\,\text{A} \times 60\,\text{sec}}{2 \times 96485\,\text{C/mol}} = 3.11 \times 10^{-5}\,\text{mol}\,. \tag{24}$$

After getting mole flow rate, it is converted to flow rate in volume flow rate by using ideal gas equation [18]:

$$P\dot{V} = \dot{m}RT \tag{25}$$
$$P = \text{Atmospheric Pressure} = 1\,\text{atm}\,,$$
$$\dot{V} = \text{Volume Flow Rate}\,(\text{L/sec})\,,$$
$$R = \text{ideal gas constant} = 0.0821\,\text{L}\cdot\text{atm/mol}\cdot\text{K}\,,$$
$$T = \text{Temperature in kelvin} = 273\,\text{K}\,,$$
$$\dot{m} = \text{molar flow rate}\,(\text{moles/sec})\,,$$
$$\dot{V} = \frac{\dot{m}RT}{P}\,, \ \dot{V}(O_2) = 0.35\,\text{ml}\,, \ \dot{V}(H_2) = 0.7\,\text{ml}\,. \tag{26}$$

For a fixed time of one minute the values of volume flow rate of both gases are determined at the current range of 1 to 12 amperes.

Figure 1 shows that the relationship between volume flow rates of gases is proportional to the current. As current increases the volume flow rate increases. This is only for pure water without the influence of any catalyst and electrolyte. It must be noted that these values are correct if there is no electrolyte, and the temperature is 273 K. To calculate the total area of the electrolyzer assembly, surface areas of rods and plates neglecting the holes in the plate are considered. Each rod has a diameter of 6 mm and a length of 10 cm.

Experiments are performed at different concentrations of alkaline KOH and by using different materials for electrode plates and rods for example stainless steel, mild steel and copper etc. Other pentameters like the orientation of the plates, gap between the plates is also

affect effect the volume of gas produced. Suitable parameters and materials are selected for the final model to produce a safe amount of gas within a specified time as well as having a good potential to withstand the corrosive environment.
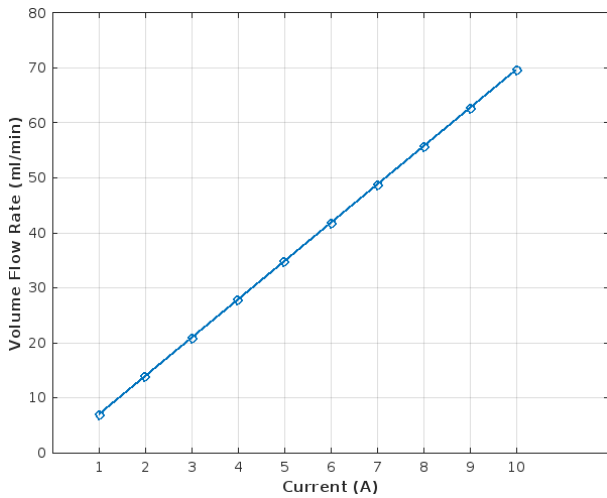

Fig. 1. Graph between current and volume flowrate.

Table 1. Electrolyzer parameters.

Diameter of rod	0.3 cm
Length of rod	10 cm
Area of rod	18.85 cm^2
Number of rods	2
Total area of rods	37.70 cm^2
Length of plates	5 cm
Width of plates	5 cm
Number of plates	14
Total area of plates	350 cm^2
Total area of assembly	387.70 cm^2

3.2 CAD model

The CAD model of the alkaline electrolyzer includes several key components: a cylindrical chamber filled with water and potassium hydroxide (KOH) as the electrolyte solution, positive and negative electrodes for facilitating electrolysis, and a steel pipe for transferring generated gases to an engine. A bubbler ensures the safe transfer of hydrogen ions, preventing engine backfire. The assembly includes steel plates arranged along M6 threaded rods to provide necessary surface area for reactions, Teflon washers are placed between the steel plates and electrodes to ensure proper spacing and electrical insulation. The CAD model shown in Figure 2 is selected to test for experimental and simulation study. The model include parallel plates configuration and the other most unique feature of this model is that the distance between the electrode plates can be increased or decreased on the basis of requirements because as we decrease the distance between the electrodes the resistance increases but the volume of gas also increases. Notably, the plates are designed so that they are not in contact with both electrodes at the same time, preventing short circuits and ensuring efficient operation. The overall design aims to maximize the electrolyzer's performance and safety.
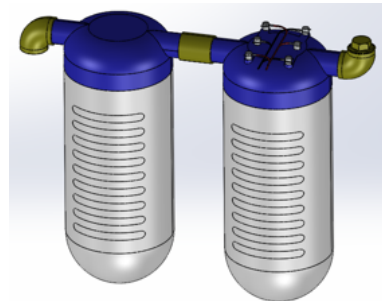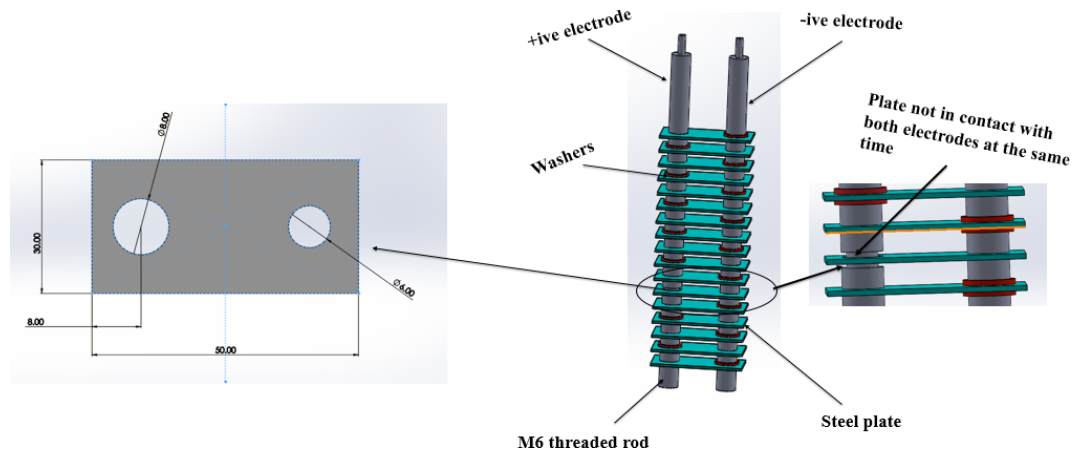

Fig. 2. Electrolyzer CAD model.

Fig. 3. A view of electrolyzer electrode.

4 Results and Discussion

4.1 Simulation results

The model is simulated in electrochemistry module in COMSOL Multiphysics. The simulation investigates the impact of gas formation on the performance of an alkaline electrolysis cell and the effect of electrolyte amount. The model was solved for different amounts of KOH, generating simulation values and current values. These simulation values were then validated through experimental data to ensure accuracy. The electrolyte used is alkaline KOH, and when the evolved gases form bubbles, the effective ionic conductivity is lowered. The generated gases may also have a detrimental effect on cell performance due to a reduced accessible surface area for the electrode reactions. For simulation the 2d model of electrode plates are simulated in COMSOL Multiphysics software the cell voltage current density and volume of gas produced at different amounts of electrolytes are simulated (Figure 4).
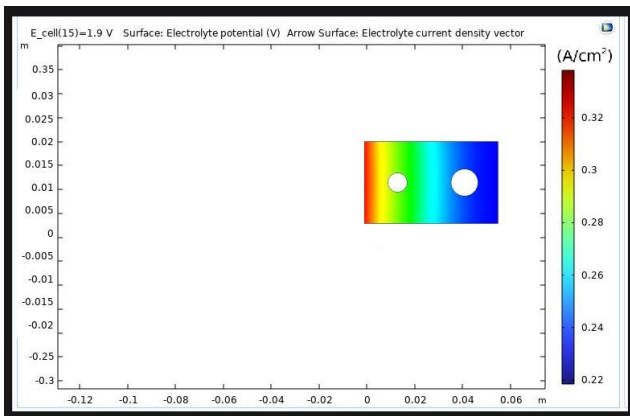

Fig. 4. Current density contours.

Form the contours of current density it can be observed higher current density near the cathode side and reduced current density at the anode side. The maximum current density is $0.0335\,\mathrm{A/cm^2}$ at 26 grams of KOH and the lowest is $0.0107\,\mathrm{A/cm^2}$ at 5 grams of electrolyte.

4.2 Experimental results of electrolyzer

Stainless steel rods and plates were selected which withstood the corrosive environment. A parallel plate configuration was employed in the experimental setup. This configuration was selected because it offers higher current density compared to other configurations. Additionally, the reduced gap between the plates minimizes gas evolution losses, thereby enhancing the overall efficiency of the electrolysis process. Potassium hy-

droxide (KOH) was chosen as the electrolyte based on findings from the literature, which indicated a significant effect when using KOH. This selection was validated through experimental data.Table summarizes the experimental results for the alkaline electrolysis process using different concentrations of KOH (potassium hydroxide) as the electrolyte. The parameters include KOH grams, percentage concentration, current (amperes), current density, voltage, volume of gas produced per minute.

Figure 5a shows a nearly linear relationship between the current and the volume flow rate indicating that as the current increases, the volume flow rate also increases proportionally this is because as we increase the amount of electrolyte the conductivity of water increases hence it demands more current and as the result the amount of gas produced also increases the influence of electrolyte amount on current can be seen in Figure 5b which shows that as the KOH concentration increases, the current also increases, indicating that higher concentrations of KOH enhance the electrolyte's conductivity, thereby allowing more current to flow through the solution.
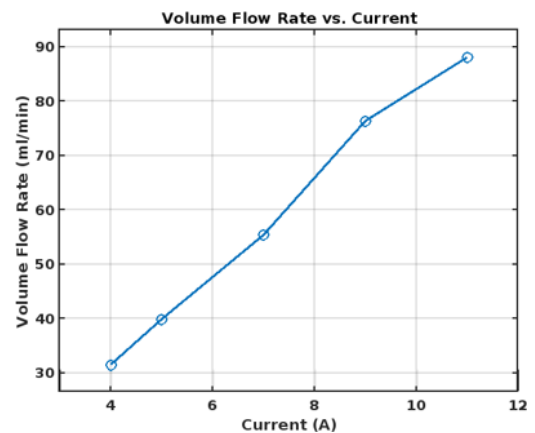

(a)
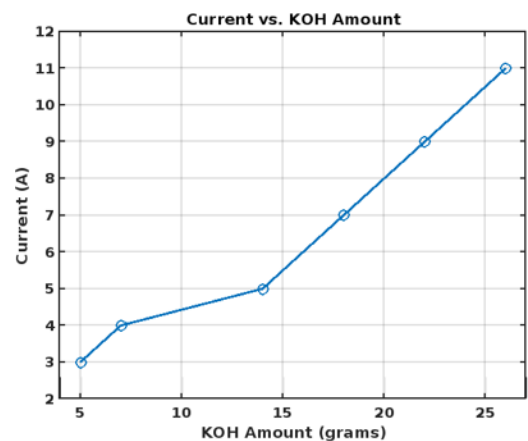
(b)

Fig. 5. Effect of KOH on current and volume of gas.

Table 2. Experimental data table.

KOH (gm)	% of KOH	Voltage (V)	Current (A)	Current density (A/cm^2)	Time (min)	Pure water theoretical	Pure water (exp)	Gas volume Alkaline water (simulated)	Gas volume Alkaline water (Experimental)
5	0.44	5.13	4	0.0103	5	27.8	30.8	37.5	35.5
7	0.53	3.3	5	0.0128	5	34.72	36.14	44.1	41.9
14	1.7	3.11	7	0.0180	5	48.81	51.91	56.13	53.33
18	1.7	5.12	9	0.0232	5	64.68	66.23	75.4	71.97
22	2	7.19	11	0.028	5	76.83	80.77	89.12	83.2
26	2.2	8	12	0.030	5	83.79	91.79	95.4	92.4

The experimental electrolysis of pure water was conducted at various currents, and the results were compared with theoretical predictions, as illustrated in Figure 6. The observed error between theoretical and experimental results ranged from 3% to 9%. This error is likely due to differences in experimental conditions: theoretical calculations assume standard conditions of 25 °C and 1 atm pressure, while the experiments were conducted at around 34 °C. Additionally, as the experiment progressed, the temperature of the electrolyzer and water increased due to resistance and current flow, leading to a slight increase in gas production. Moreover, the continuous production of gas raised the pressure within the electrolyzer, as the generated gas exerted vapor pressure on the water, contributing to the observed error.
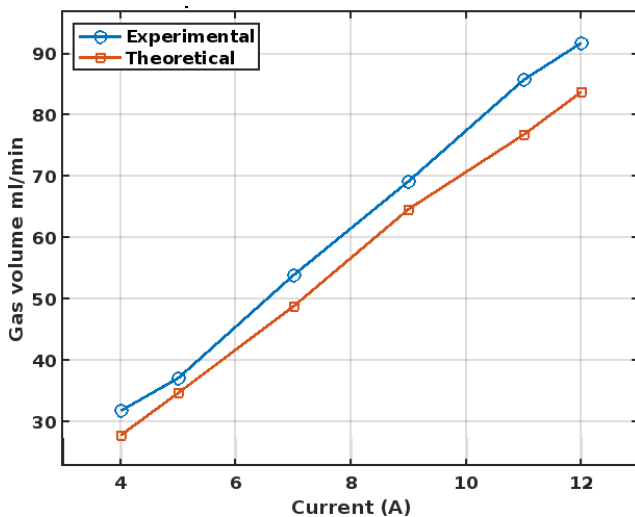
Fig. 6. Graph theoretical and experimental results of pure water.

In Figure 7 a graph between experimental volume of gas produced in a particular time is measured and compared with simulation results the error ranges from 4 to 6 percent and is acceptable with the possible reasons of temperature and pressure variations and small

leakages of gas during the measuring process that's the possible reason of decreased amount of experimental volume in experimental analysis.
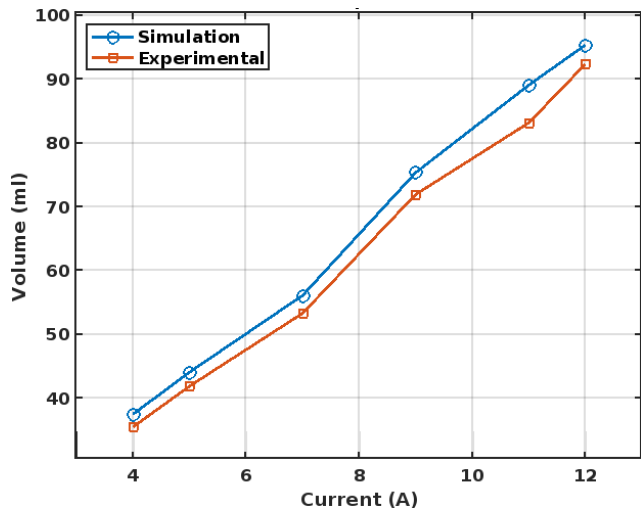

Fig. 7. Graph between experimental and simulation results of alkaline water.

Figure 8 shows a linear relationship between increasing electrolyte concentration and current density. This trend occurs because higher electrolyte concentrations increase ion availability, reducing electrical resistance and allowing more current to flow through the solution for a given voltage, thus raising the current density. In Figure 9 a comparison between simulation and experimental voltage is show in which initially, increasing KOH concentration lowers cell voltage by reducing solution resistance and enhancing conductivity. However, beyond a certain concentration, the voltage starts to increase due to higher viscosity, ion interference, and potential side effects, which raise internal resistance.

Figure 10 represents the effect of temperature on current density as temperature increases during electrolysis, current density rises due to several factors. Higher temperatures enhance ionic conductivity by re-

ducing the electrolyte's viscosity and increasing ion mobility, which lowers the solution's electrical resistance. This allows more current to flow through the electrolyte for a given voltage.
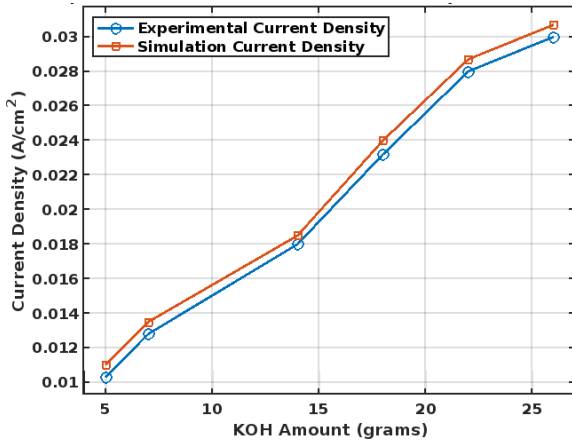
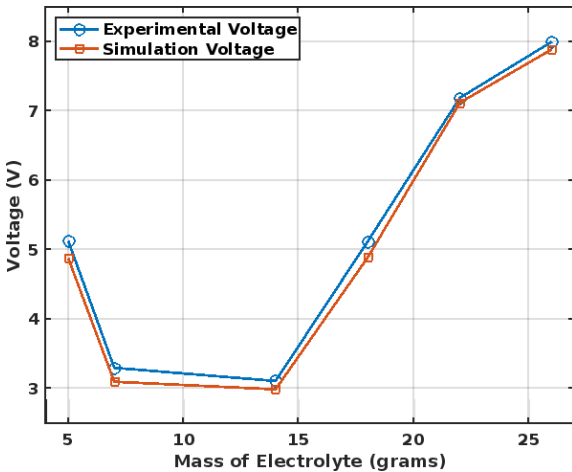**Fig. 8. Graph between simulation and experimental current density.**
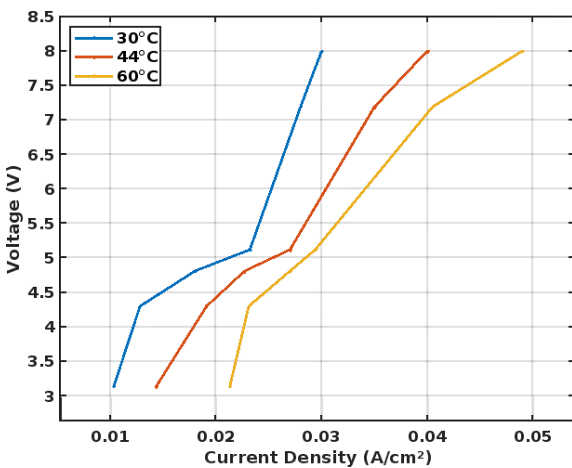
Fig. 9. Comparison of voltage.

Fig. 10. Effect of temperature on current density.

Figure 11 shows the current densities of different electrodes, stainless steel proved to be the most feasible electrode material due to its corrosion resistance and higherst current density. In contrast, while copper exhibited good current density due to its excellent conductivity, it suffers from lower corrosion resistance, which can compromise its performance and longevity. Mild steel, although it is cost-effective, had the lowest current density and higher susceptibility to corrosion, making it less suitable for electrolysis applications where durability and efficiency are critical.
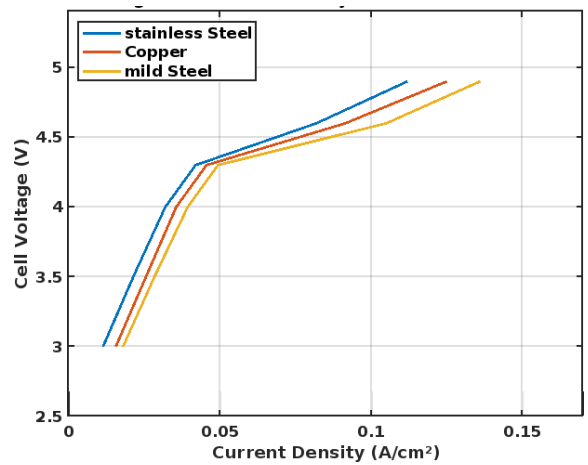
Fig. 11. Effect of electrode material on current density.

5 Conclusion

The pressing need for renewable energy alternatives underscores the significance of hydrogen energy, particularly when generated from sustainable sources such as solar power. This study explored the design, simulation, and experimental evaluation of a solar-powered alkaline electrolyzer, focusing on optimizing hydrogen and oxygen production through controlled electrolysis. Our detailed mathematical modeling provided insights into the electrolysis process, accounting for various losses and optimizing design parameters. The experimental analysis revealed that varying potassium hydroxide (KOH) concentrations and elevated temperatures significantly impacted gas output. Stainless steel electrodes demonstrated superior performance due to their corrosion resistance, while a parallel plate configuration was chosen for its efficiency in current density and reduced gas evolution losses. Experimental results aligned well with theoretical predictions, though slight discrepancies were noted, attributed to variations in experimental conditions such as temperature and pressure. These variations contributed to minor differences in gas production rates and volumes. Additionally,

the study observed that increasing electrolyte concentration improved current density by reducing electrical resistance, although excessive concentrations led to higher cell voltage due to increased viscosity and ion interference. Temperature also played a crucial role, with higher temperatures enhancing current density by improving ionic conductivity. Among the electrode materials tested, stainless steel emerged as the most effective, combining corrosion resistance with high current density. Conversely, copper, despite its high conductivity, was less suitable due to corrosion issues, and mild steel, while cost-effective, proved less efficient due to its low current density and susceptibility to corrosion Overall, this study confirms the viability of using solar-powered alkaline electrolyzer's for hydrogen production and highlights critical factors such as electrolyte concentration, temperature, and electrode material in optimizing electrolysis performance.

References

[1] Wang J, Azam W. Natural resource scarcity, fossil fuel energy consumption, and total greenhouse gas emissions in top emitting countries. Geoscience Frontiers. 2024;15(2):101757. Available from: https://www.sciencedirect.com/science/article/pii/S1674987123002244.

[2] Holechek JL, Geli HME, Sawalhah MN, Valdez R. A Global Assessment: Can Renewable Energy Replace Fossil Fuels by 2050? Sustainability. 2022;14(8). Available from: https://www.mdpi.com/2071-1050/14/8/4792.

[3] Chi J, Yu H. Water electrolysis based on renewable energy for hydrogen production. Chinese Journal of Catalysis. 2018;39(3):390–394. Available from: https://www.sciencedirect.com/science/article/pii/S1872206717629498.

[4] Hren R, Vujanović A, Van Fan Y, Klemeš JJ, Krajnc D, Čuček L. Hydrogen production, storage and transport for renewable energy and chemicals: An environmental footprint assessment. Renewable and Sustainable Energy Reviews. 2023;173:113113. Available from: https://www.sciencedirect.com/science/article/pii/S1364032122009947.

[5] Bratsch SG. Standard Electrode Potentials and Temperature Coefficients in Water at 298.15 K. Journal of Physical and Chemical Reference Data. 1989 01;18(1):1–21. Available from: https://doi.org/10.1063/1.555839.

[6] Ursúa A, San Martín I, Barrios EL, Sanchis P. Stand-alone operation of an alkaline water electrolyser fed by wind and photovoltaic systems. International Journal of Hydrogen Energy. 2013;38(35):14952–14967. Available from: https://www.sciencedirect.com/science/article/pii/S0360319913023082.

[7] Tjarks G, Mergel J, Stolten D. In: Dynamic Operation of Electrolyzers - Systems Design and Operating Strategies; 2016. p. 309–330.

[8] Schalenbach M, Carmo M, Fritz DL, Mergel J, Stolten D. Pressurized PEM water electrolysis: Efficiency and gas crossover. International Journal of Hydrogen Energy. 2013;38(35):14921–14933. Available from: https://www.sciencedirect.com/science/article/pii/S0360319913022040.

[9] Schröder V, Emonts B, Janßen H, Schulze HP. Explosion Limits of Hydrogen/Oxygen Mixtures at Initial Pressures up to 200 bar. Chemical Engineering & Technology. 2004;27(8):847–851. Available from: https://onlinelibrary.wiley.com/doi/abs/10.1002/ceat.200403174.

[10] Hug W, Divisek J, Mergel J, Seeger W, Steeb H. Highly efficient advanced alkaline electrolyzer for solar operation. International Journal of Hydrogen Energy. 1992;17(9):699–705. Available from: https://www.sciencedirect.com/science/article/pii/036031999290090J.

[11] Kothari R, Buddhi D, Sawhney RL. Comparison of environmental and economic aspects of various hydrogen production methods. Renewable and Sustainable Energy Reviews. 2008;12(2):553–563. Available from: https://www.sciencedirect.com/science/article/pii/S1364032106001158.

[12] David M, Ocampo-Martínez C, Sánchez-Peña R. Advances in alkaline water electrolyzers: A review. Journal of Energy Storage. 2019;23:392–403. Available from: https://www.sciencedirect.com/science/article/pii/S2352152X18306558.

[13] Ishaq H, Dincer I. Comparative assessment of renewable energy-based hydrogen production methods. Renewable and Sustainable Energy Reviews. 2021;135:110192. Available from: https://www.sciencedirect.com/science/article/pii/S1364032120304822.

[14] Boretti A. Hydrogen internal combustion engines to 2030. International Journal of Hydrogen Energy. 2020;45(43):23692–23703. Available from: https://www.sciencedirect.com/science/article/pii/S0360319920321595.

[15] Zareei J, Mahmood F, Abdullah S. Theoretical study of the effect of hydrogen addition to natural gas-fueled direct-injection engines. Hydrogen, Fuel Cell & Energy Storage. 2014;1(1):11–20. Available from: https://hfe.irost.ir/article_9.html.

[16] Haverkort JW, Rajaei H. Voltage losses in zero-gap alkaline water electrolysis. Journal of Power Sources. 2021;497:229864. Available from: https://www.sciencedirect.com/science/article/pii/S037877532100402X.

[17] Wilcox GD, Gabe DR. Faraday's Laws of Electrolysis. Transactions of the IMF. 1992;70(2):93–94. Available from: https://doi.org/10.1080/00202967.1992.11870951.

[18] Laugier A, Garai J. Derivation of the Ideal Gas Law. Journal of Chemical Education. 2007;84(11):1832. Available from: https://doi.org/10.1021/ed084p1832.